INTERNATIONAL JOURNAL FOR NUMERICAL METHODS IN FLUIDS, VOL. 14, 1421–1436 (1992)

A CODING ERROR ELIMINATION PROCEDURE FOR VALIDATING ISOTROPIC TURBULENT CONVECTION NUMERICAL CALCULATIONS IN AXISYMMETRIC FLOWS WITH EULERIAN AND LAGRANGIAN DESCRIPTIONS

DAVID A. BLANK

Mechanical Engineering Department, U.S. Naval Academy, Annapolis, MD 21402, U.S.A.

SUMMARY

A procedure which ensures the elimination of discretization and coding errors in the numerical solution of a set of governing equations describing internal turbulent convection flows is given and illustrated. The governing equations investigated in the validation analysis are of general form. The equations for the turbulence model (k–ε) assume the turbulence to be isotropic. In the analysis a portion of the solution region uses a Lagrangian description while a Eulerian description is used elsewhere. The work was originally motivated by the need to validate numerical calculations performed in the modelling of combusting fluid flow within symmetric piston engines. Thus the procedure is demonstrated for an axisymmetric formulation. The same methodology can be even more easily applied to Cartesian-based problems using the guidelines given in this work. Details of the procedure are presented in a very practical format, making it possible to consider both simpler and more complex governing equation sets with little additional effort. Thus the implementation of this procedure by researchers to a variety of both turbulent and laminar internal flow problems should prove to be easy.

KEY WORDS Error elimination Debugging Combined Eulerian–Lagrangian description Fluid flow Turbulent flow Convective heat transfer Computational methods Numerical methods Numerical heat transfer

1. INTRODUCTION

In general, unsteady non-reacting isotropic turbulent convection flows in axisymmetric co-ordinates require the simultaneous solution of six or more non-linear differential equations, depending on the complexity of the turbulence model. If swirl is neglected and a k–ε model is employed to account for the turbulence, the number of equations required is six.[1] For internal flows with radiation heat transfer neglected, each of these six equations will have an average of approximately eight expressions.[2] Depending on the equation, some of these expressions will themselves contain multiple terms. Assuming that these general governing equations have been properly derived and appropriately modified for a given application, three major tasks remain in order to obtain a numerical solution. The first is the discretization of each of the terms in the expressions for all six governing equations. This task can be simplified somewhat by arranging the convection and diffusion portions of these equations in a common format. The resultant algebraic expressions must then be properly coded into a computer solution algorithm. Lastly, the boundary conditions and various fluid properties must be properly specified in the code.

0271–2091/92/121421–16$08.00

Received 15 July 1991
Revised 30 October 1991

Once a convergent solution has been obtained using the resultant code, the question remains as to the validity of the computation. If either experimental data are available or high quality numerical results from other works exist for a flow scenario appropriate to the governing equations utilized, a qualitative analysis of the new code can be made. Favourable comparison of the code configured to solve such a problem (or problems) does not, however, guarantee that errors have not been made. The relative contribution of each term in the governing equations will change when the code is applied to other problems. An error in discretization or coding may not show up for the comparison case (or cases) chosen. Obviously, a more reliable procedure is needed to ensure that all errors are found and eliminated.

The particulars of the verification procedure contained herein were developed in support of a much larger study[2-4] using a method first formally formulated by Shih.[5] The work was conducted to confirm the integrity of a computational scheme developed to model the conjugate conduction–convection processes taking place in a heat barrier piston internal combustion engine with a fully functional valve. The problems associated with representing the thermal characteristic of a moving valve while also handling the conjugate heat exchange between a fluid flow field region and a metal non-flow region (with the exterior temperature boundary conditions specified) resulted in the creation of a number of special requirements. This combination of requirements further resulted in, among other things, a three-region approach.[4] In regions 1 and 3, shown in Figure 1, a Eulerian description is applicable. In region 1 the position of all solution nodal points is fixed in space and time. In region 3 the motion of all solution nodal points is slaved to the piston motion and they move without distortion relative to one another. In region 2 the mesh is stretched and compressed in accordance with the piston motion and has

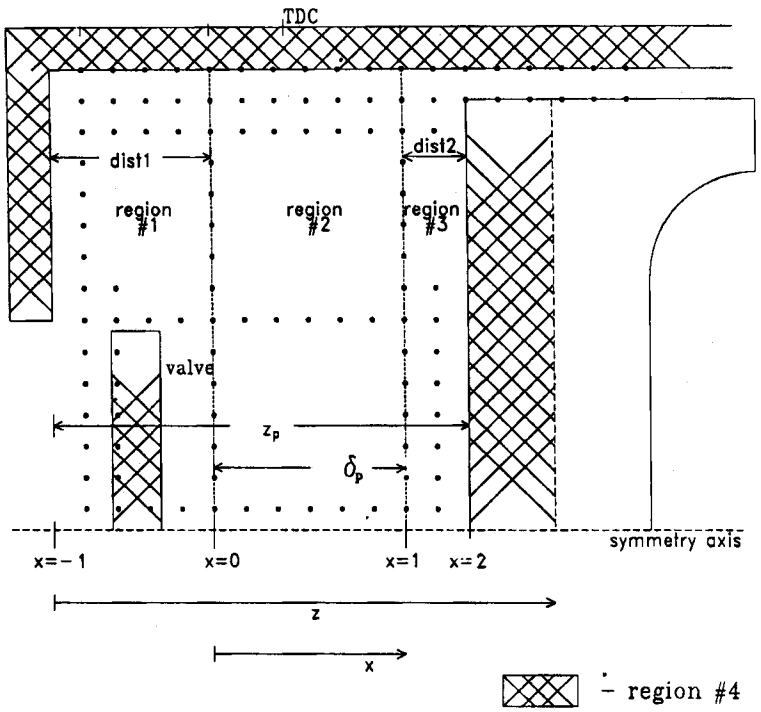

Figure 1. Solution regions

instead a Lagrangian description. Both the interfaces between regions 1 and 2 and between regions 2 and 3 required the development of a special matching procedure.[4] Thus the original aims of the analysis described herein were twofold: (1) the validation of several of the innovations required to solve the problem described above and (2) the verification of the integrity of the resultant solution code.

Results of a preliminary validation analysis with the above two aims in mind are contained in References 6 and 7. Considered in this earlier study was the computation of the primitive variables u, v, k, ε and T subject to a constant pressure flow field. Thus the integrity of the pressure correction scheme was not investigated. The procedure presented herein, however, includes a method for the validation of a pressure correction scheme for pressure fields that vary both spatially and with time.

FORMULATION AND GOVERNING EQUATIONS

A precise mathematical formulation of the general procedure employed herein to analyse error is contained in Reference 5. The essence of this procedure is also briefly described in verbal terms in Reference 8. The following paragraphs present a formulation equivalent to Reference 5 mathematically and yet very different in format to accommodate the nomenclature in use in References 2–4.

In axisymmetric co-ordinates, isotropic turbulent convection with swirl neglected requires in general a coupled set of six partial differential equations to adequately account for turbulence, energy, linear momentum and continuity. Each of the equations in this set has the same general form and is represented compactly below by the general transport equation in terms of the primitive varible ϕ:[2]

$$\frac{1}{\delta_p}\frac{\partial}{\partial t}(\rho\delta_p\phi)+\frac{1}{\delta_p}\frac{\partial}{\partial x}(\rho\bar{u}\phi)+\frac{1}{r}\frac{\partial}{\partial r}(r\rho v\phi)=\frac{1}{\delta_p}\frac{\partial}{\partial x}\left(\frac{\Gamma_\phi}{\delta_p}\frac{\partial\phi}{\partial x}\right)+\frac{1}{r}\frac{\partial}{\partial r}\left(r\Gamma_\phi\frac{\partial\phi}{\partial r}\right)+\bar{S}_\phi, \tag{1}$$

where ϕ can be either 1, u, v, k, ε or T. Equation (1) is a Lagrangian description of the flow applicable to piston engines and is a transformed version of the general Eulerian-based governing equations. The expression $\bar{u}$ is equal to $u-xu_p$, where x is the non-dimensional axial co-ordinate in Figure 1. The term δ_p is the axial length of region 2 (Figure 1) and is a function of time. The term u_p is equal to $d\delta_p/dt$ and represents the velocity of the piston. Equation (1) has utility in region 2 as expressed. Its utility in region 1 is obtained by setting u_p equal to zero and δ_p equal to dist1. Similarly, its utility in region 3 is obtained by setting δ_p equal to dist2 and leaving $u_p=u_p$. A summary of the $\bar{S}_\phi$ and Γ_ϕ applicable to each ϕ is given in Table I. In regions 1 and 3 the 'untransformed' source term S_ϕ can be obtained from those given in Table I using the same specifications given above for these two regions.

References 6 and 7 give a description of the discretization of the general transformed flow field transport equation (equation (1)) along with details of the discretization of each of the source terms contained in Table I. For this discretization a staggered grid arrangement is employed with the faces of the control volume midway between nodal points. For the work in References 2–4 and herein the power-law spatial-differencing scheme[8] for the approximation of the convection–diffusion flux terms is used. Finally, implicit differencing in time is used. The resulting set of algebraic equations representing the transformed general transport equation for the primitive variable ϕ becomes

$$(a_p+M^0-\bar{S}_p)\phi=\sum_m a_m\phi_m+\bar{S}_u+M^0\phi^0, \tag{2}$$

Table I. Transformed governing equation source terms

Equation	ϕ	Γ_ϕ	$\bar{S}_\phi$
Continuity	1	0	0
Axial momentum	u	μ_{eff}	$-\frac{1}{\delta_p}\frac{\partial P}{\partial x}+\frac{1}{\delta_p}\frac{\partial}{\partial x}\left(\frac{\mu_{\text{eff}}}{\delta_p}\frac{\partial u}{\partial x}\right)+\frac{1}{r}\frac{\partial}{\partial r}\left(\frac{r\mu_{\text{eff}}}{\delta_p}\frac{\partial v}{\partial x}\right)-\frac{2}{3\delta_p}\frac{\partial}{\partial x}(\mu_{\text{eff}}\nabla\cdot\mathbf{u}+\rho k)$
Radial mo……um	v	μ_{eff}	$-\frac{\partial P}{\partial r}+\frac{1}{\delta_p}\frac{\partial}{\partial x}\left(\mu_{\text{eff}}\frac{\partial u}{\partial r}\right)+\frac{1}{r}\frac{\partial}{\partial r}\left(r\mu_{\text{eff}}\frac{\partial v}{\partial r}\right)$ $-2\mu_{\text{eff}}\frac{v}{r^2}-\frac{2}{3}\frac{1}{r}\frac{\partial}{\partial r}[r(\mu_{\text{eff}}\nabla\cdot\mathbf{u}+\rho k)]$
Turbulence kinetic energy	k	$\frac{\mu_{\text{eff}}}{\sigma_k}$	$-C_D\rho\varepsilon+\bar{G}$ (see transformed G below)*
Turbulence kinetic energy dissipation rate	ε	$\frac{\mu_{\text{eff}}}{\sigma_\varepsilon}$	$\frac{\varepsilon}{k}(C_1\bar{G}-C_2\rho\varepsilon)+\rho\varepsilon\nabla\cdot\mathbf{u}$
Energy	T	γ_{eff}	$\frac{1}{C_p}\left(\frac{\partial P}{\partial t}-\frac{x}{\delta_p}u_p\frac{\partial P}{\partial x}+\frac{u}{\delta_p}\frac{\partial P}{\partial x}+v\frac{\partial P}{\partial r}+\bar{G}\right)$

* $\bar{G}=2\mu_{\text{eff}}\left[\left(\frac{1}{\delta_p}\frac{\partial u}{\partial x}\right)^2+\left(\frac{\partial v}{\partial r}\right)^2+\left(\frac{v}{r}\right)^2+\frac{1}{2}\left(\frac{\partial u}{\partial r}+\frac{1}{\delta_p}\frac{\partial v}{\partial x}\right)^2\right]-\frac{2}{3}\nabla\cdot\mathbf{u}(\mu_{\text{eff}}\nabla\cdot\mathbf{u}+\rho k)$

$\nabla\cdot\mathbf{u}=\frac{1}{\delta_p}\frac{\partial u}{\partial x}+\frac{v}{r}+\frac{\partial v}{\partial r}$, $\mu_{\text{eff}}=\mu_l+C_\mu\rho\frac{k^2}{\varepsilon}$, $\gamma_{\text{eff}}=\frac{\mu_l}{Pr_l}+\frac{C_\mu}{Pr_t}\rho\frac{k^2}{\varepsilon}$

where $m=$ N, S, E, W, $a_p=\sum_m a_m$, a_m is defined in detail in Reference 3, $M^0=(\rho V/\Delta t)^0$, superscript 'o' indicates the previous ('old') time step and V is the volume of the control volume in question.

For each primitive variable ϕ equation (2) thus represents an algebraic approximation of the general governing transport equation (1). It would be nice if a series of analytical expressions for all the ϕs could be found in order to test the validity of using equation (2) as an approximation of equation (1) for each ϕ. In the real world, however, an analytical solution does not exist for equation (1) for any of its primitive variables. Despite this fact, for the purpose of analysing the equivalence of equation (2) to equation (1), it will be assumed that the primitive variables u, v, k, ε and T can be quantified analytically in such a way so as to satisfy a modified version of equation (2). Similarly, the combination of the u- and v-momentum equations and the continuity equation will be assumed to support an analytical expression for the variable P. In general it is assumed that

$$\phi=\phi(x, r, t), \tag{3}$$

subject to Dirichlet boundary conditions for all ϕ. For clarity, Dirichlet boundary conditions are obtained from the analytical expressions for the various ϕs evaluated at the boundary. For the continuity equation ϕ will still equal unity. P, however, will equal $P(x, r, t)$ and will be solved for numerically using the continuity equation. Pressure will thus be considered the sixth primitive variable instead. Obviously, no combination of $\phi=\phi(x, r, t)$ for all six primitive variables exists that can be used to simultaneously solve the six equations represented by equation (1) or equation (2). However, the correct selection of $\phi=\phi(x, r, t)$ for all six variables can be used to simultaneously satisfy the six equations represented by the modification of equation (2) given below:

$$(a_p+M^0-\bar{S}_p)\phi=\sum_m a_m\phi_m^n+\bar{S}_u+M^0\phi^0+CR_{\text{anal}_\phi}V_\phi, \tag{4a}$$

where

$$C=\begin{cases}1 & \text{when error analysis utilized in computer code subject to Dirichlet boundary conditions,}\\ 0 & \text{for solution of real problem subject to boundary conditions specified in References 2–4,}\end{cases} \tag{4b}$$

$$R_{\text{anal}_\phi} \equiv H\phi(x,r,t)-\bar{S}_\phi(x,r,t), \tag{4c}$$

$$H\phi \equiv \frac{1}{\delta_p}\frac{\partial}{\partial t}(\rho\delta_p\phi)+\frac{1}{\delta_p}\frac{\partial}{\partial x}\left(\rho\bar{u}\phi-\frac{\Gamma_\phi}{\delta_p}\frac{\partial\phi}{\partial x}\right)+\frac{1}{r}\frac{\partial}{\partial r}\left(r\rho v\phi-r\Gamma_\phi\frac{\partial\phi}{\partial r}\right). \tag{4d}$$

Thus R_{anal_ϕ} is obtained by simultaneously substituting the $\phi(x,r,t)$ expressions for all six primitive variables into *each* of the six equations represented by equation (4c). In effect the $\phi(x,y,t)$ expressions become the solutions to the new set of six equations represented by equation (4a) subject to Dirichlet boundary conditions on all geometric boundaries and on the previous time step boundary. These primitive variable expressions will also satisfy a modified version of equation (1), namely

$$H\phi=\bar{S}_\phi+R_{\text{anal}_\phi}. \tag{5}$$

It should be noted that these $\phi(x,r,t)$ expressions thus represent a set of particular solutions for the equation set represented by equation (5) and may therefore be loosely referred to as analytical solutions for the same. Discretization of equation (5) in a manner identical to the discretization of equation (1) will result in equation (4a) with $C=1$. The numerical solution of equation (5) for Dirichlet boundary conditions specified both for all geometric boundaries and for the initial time boundary can thus be obtained through the solution of equation (4a) subject to these same boundary conditions. The results of this numerical solution are values that can be compared with the known solution, namely $\phi(x,y,t)$, for each primitive variable.

For comparison with R_{anal_ϕ} for various ϕs, an expression for R_{num_ϕ} was also derived using equation (4a) with $C=1$:

$$R_{\text{num}}=\frac{1}{V_\phi}\left[(a_p+M^0-\bar{S}_p)\phi-\left(\sum_m a_m\phi_m+\bar{S}_u+M^0\phi^0\right)\right]. \tag{6}$$

It should be noted that the above formulation is only able to test the accuracy of the discretization and coding process for each of the six governing equations. It does not provide a means for testing the specification and coding of the wall functions in References 2–4 used as boundary conditions. With the expression R_{anal_ϕ} added to the source term, the governing equations (4) are altered such that they are valid right up the 'wall' of the solution scheme where Dirichlet values are specified. It should be further noted that it is the integrity of both the discretization of the governing equations and the coding of the algebraic expressions that results from this discretization process that is being tested. It is *not* the testing of the validity of the governing equations themselves that is under scrutiny in the present analysis.

APPLICATION TO THE TURBULENT CONVECTION PROBLEM

The specification of $\phi(x,r,t)$ for use in the validation of the scheme used in the solution of the particular set of governing equations given in the previous section is by no means an arbitrary process. As alluded to in Reference 5, these expressions should in general be chosen so that the truncation errors associated with a finite difference formulation vanish or are at least sufficiently

small. This puts upper limits on the powers of the terms used to construct each function. On the other hand, it is desirable that the functions chosen be made up of terms with high enough powers that they do not vanish when substituted into their respective governing equations. If they do vanish, it should only be either the result of the final differentiation of the function in one of the higher-order differential expressions or the result of the algebraic summations of several sub-expressions. Additionally, the function set must be designed in such a way so as to ensure that the functions interact with each other in the governing equations in a 'reasonable' manner. It was found that if the construction of one or more functions in the function set is unrealistic compared to others, equation (4a) either may not converge or may converge to incorrect values.

As an example of the implementation of the above guidelines, consider the selection of the primitive variable P. The dominant source term in the u-momentum equation is often $-\partial P/\partial x$ for internal flows. The dominant convection–diffusion term is expected to be $\partial(\rho\bar{u}u)/\partial x$. A selection of analytical expressions for P and u which reasonably satisfy these dominant terms is preferable if convergence to correct values is to be guaranteed. Also, if the discretization used for $\partial P/\partial x$ gives a third-order truncation error (as it does in the case of a staggered grid), the highest power of x in $P(x, r, t)$ must not be greater than four. This determination will guarantee the truncation error $(\Delta x/2)^2\partial^3 P/\partial x^3$ to be sufficiently small for reasonably fine grid spacing. All the above is also true for the modelling of P relative to the v-momentum equation. In the energy equation P is used, among other places, in the $\partial P/\partial t$ term. When considering the Lagrangian formulation of the energy equation, the change in P with time must be of the same power of exponent for t as the change in the size of the energy equation control volume (V_T) with time. The size of V_T is in turn a function of $\delta_p(t)$. To ensure convergence to correct values, the order of the exponent associated with time t in the specification of P must thus contain the use of the same order of exponent of t as is used in the specification of $\delta_p(t)$. In Reference 4, δ_p in region 2 is specified as a trigonometric function which accounts for piston motion. For this error test, however, it was found necessary to respecify δ_p in region 2 as an expression containing powers of t in order to make possible a correctly coupled expression for P. This combination of constraints along with others were all involved in the specification of $P(x, r, t)$ relative to the selection of $T(x, r, t)$, $\delta_p(t)$, $u(x, r, t)$ and $v(x, r, t)$.

Using the same type of analysis for the other primitive variables, the following specifications for ϕ were arrived at after significant analytical work and much trial and error:

$$u \equiv tx^2r, \tag{7}$$

$$v \equiv -\tfrac{2}{3}txr^2, \tag{8}$$

$$k \equiv C_6xr(x+r)t, \tag{9}$$

$$\varepsilon \equiv C_6^2x^2r^2tC_7, \tag{10}$$

$$P \equiv \frac{C_8C_{10}t^2}{4R}(\tfrac{5}{9}x^2r^4 - x^4r^2) + 3C_8, \tag{11}$$

$$T \equiv -C_9tx^2r^2 + 3C_9, \tag{12}$$

where C_6, C_7, C_8, C_9 and C_{10} are constants (specified as 0·75, 0·8888, 500, 500 and 1000 respectively). Although these functions all tend to infinity in magnitude as time approaches infinity, they are only intended for use in relatively close vicinity to t^n.

The selection of

$$\rho = C_{10}/R \tag{13}$$

was made corresponding to the assumption of a constant density fluid with a gas constant R.

Specification of ρ as a function of x, r and t instead would greatly and unnecessarily complicate the R_{anal_ϕ} expressions. It should be noted that the selection of equation (13) for an equation of state also serves to decouple all the other governing equations from the energy equation. This is because this specification has the effect of making the fictitious test flow incompressible. In References 2–4, which deal with a real world problem, density is specified as a function of T, P and various species concentrations. Thus in References 2–4 all the governing equations are coupled. The equation (13) specification for density results in an average value which falls within the range of those expected for this property in the real calculations given in References 2–4.

Piston motion for the error analysis within region 2 was specified as the increasing function

$$\delta_p(t^n) = C_{11}t^0 + C_{12}(t^n)^2, \tag{14}$$

where C_{11} and C_{12} are constants equal to 0·0014826 and 0·0081545 respectively. Note that the superscript 'o' on the first t indicates the old time value of t. In regions 1 and 3 the expression $\delta_p(t^n)$ was set equal to the constant values dist1 and dist2 respectively.

The values chosen for the seven constants C_6–C_{12} are based on several considerations. First, they ensure that the resultant values of all $\phi(x, r, t)$ and δ_p are all reasonable over the range of x and r and the domain of t used in the test. Also, they help to enable a realistic interrelationship between these variables. An attempt was made to have values for the various ϕs within the range of values expected in 'real' calculations.[2–4]

It should be noted that in the construction of equation (7) in conjunction with equation (8) it was necessary to satisfy the transformed continuity equation. Further, these two specifications define a vector field which is well out of alignment with both the axial and radial axes when values of x and r are sufficiently close in magnitude. The latter is preferable in providing a good test for the power-law convection–diffusion flux discretization formulation used in the analysis.[3] Finally, it should be noted that these specifications give algebraic expressions for $\nabla \cdot \mathbf{u}$ which cancel to zero. Since $\nabla \cdot \mathbf{u}$ expressions exist in four of the governing equations, this greatly simplifies the algebra of the resulting R_{anal_ϕ} for these equations.

Substitution of equations (7)–(13) into equation (4c) resulted in the expressions for R_{anal_ϕ} for the five ϕs summarized in Table II. $H\phi$ for the continuity equation is equal to zero, as is its source term. Boundary conditions for the error analysis are depicted in Figure 2. It should also be noted that because of the pressure correction in the solution of the continuity equation, it was also necessary to prespecify the analytical value for the pressure at one of the interior nodal points to serve as a pressure reference point. Whether such a specification is necessary or not is dependent on the algorithm used to solve for the pressure field. In the analysis conducted in References 2–4 a pressure correction procedure was used to obtain the pressure field. In such an approach the continuity equation does not make use of the Dirichlet boundary conditions for pressure directly. It does use these conditions indirectly and they are also used directly in the computations for u, v, T and P. In the exercise herein the equation of state is $\rho = \text{const}$ (equation (13)). If ρ were instead a function of T, P and other variables, the pressure correction scheme employed would not need a prespecified reference point. However, allowing ρ to equal $\rho(P, T)$, for example, would, as mentioned earlier, result in much more complicated expressions for R_{anal_ϕ} than those given in Table II.

The use of the above formulation in a flow field with a combined Eulerian–Lagrangian description was found to require a special approach. It was found that in general it is simpler and more computationally efficient to solve regions 1, 2 and 3 together as opposed to solving in an iterative manner back and forth between each. When solving all regions together, the use of $\phi = \phi(x, r, t)$, is however, complicated by the fact that the transformation for the dimensional axial co-ordinate (z) to the non-dimensional axial co-ordinate (x) varies with region. The

Table II. R_{anal} for various primitive variables ($H\phi - \bar{S}_\phi$)

ϕ	$H\phi$	$\bar{S}_\phi$
u	$\frac{1}{R_1}(x^2r+\frac{4}{3}t^2x^3r^2)-(a+b(x+r)^2)$ $\times\left(2tr+t\frac{x^2}{r}\right)-b(x+r)(4xr+2x^2)t$	$-\frac{\partial P}{\partial x}+2b(x+r)(2xr-\frac{2}{3}r^2)t-\frac{2}{3}\frac{C_6}{R_1}(2xr+r^2)t$
v	$\frac{1}{R_1}(-\frac{2}{3}xr^2+\frac{2}{9}t^2x^2r^3)+(a+b(x+r)^2(\frac{8}{3}tx)$ $+b(x+r)(\frac{4}{3}r^2+\frac{8}{3}xr)t$	$-\frac{\partial P}{\partial r}+[a+b(x+r)^2]\frac{2}{3}tx+2b(x+r)(x^2-\frac{4}{3}xr)t$ $-\frac{2}{3}\frac{C_6}{R_1}(2x^2+3xr)t$
k	$\frac{C_6}{R_1}(xr(x+r)+t^2x^2r^2(\frac{4}{3}x-\frac{1}{3}r))$ $-(a_1+b_1(x+r)^2)\left(4x+\frac{x^2}{r}+2r\right)C_6t$ $-2b_1(x+r)(x^2+4xr+r^2)C_6t$	$-\frac{C_D}{R_1}C_6^2x^2r^2tC_7+\bar{G}$ (see transformed G below)*
ε	$\left[\frac{1}{R_1}(x^2r^2+\frac{2}{3}t^2x^3r^3)\right.$ $-(a_2+b_2(x+r)^2(r^2+2x^2)2t$ $\left.-2b_2(x+r)(xr^2+x^2r)2t\right]C_6^2C_7$	$\frac{C_6xrC_7}{x+r}\left(C_1\bar{G}-\frac{C_2}{R_1}C_6^2x^2r^2tC_7\right)$
T	$-\frac{1}{R_1}(x^2r^2+\frac{2}{3}t^2x^3r^3)C_9$ $+\frac{1}{C_p}(a_3+b_3(x+r)^2(r^2+2x^2)2tC_9$ $+\frac{2}{C_p}b_3(x+r)(xr^2+x^2r)2tC_9$	$\frac{1}{C_p}\left(\frac{\partial P}{\partial t}+v\frac{\partial P}{\partial r}+u\frac{\partial P}{\partial x}+\bar{G}\right)$

* $\bar{G}=2[a+b(x+r)^2](\frac{1}{2}x^4+\frac{10}{9}x^2r^2+\frac{2}{9}r^4)t^2$

$a=\mu_l$, $a_1=\frac{\mu_l}{\sigma_k}$, $a_2=\frac{\mu_l}{\sigma_\varepsilon}$, $a_3=\frac{\mu_l}{Pr_l}$

$b=\frac{C_\mu}{R_1C_7}t$, $b_1=\frac{C_\mu t}{R_1C_7\sigma_k}$, $b_2=\frac{C_\mu t}{R_1C_7\sigma_\varepsilon}$, $b_3=\frac{C_\mu t}{R_1Pr_tC_7}$, $R_1=\frac{R}{C_{10}}$

$\frac{\partial P}{\partial x}=(\frac{10}{9}xr^4-4x^3r^2)\frac{t^2C_8}{2R_1}$, $\frac{\partial P}{\partial r}=(\frac{20}{9}x^2r^3-2x^4r)\frac{t^2C_8}{2R_1}$, $\frac{\partial P}{\partial t}=(\frac{5}{9}x^2r^4-x^4r^2)\frac{tC_8}{R_1}$

expression of x for each region in terms of z is as follows:

region 1, $$x=\frac{z}{\text{dist1}}-1{\cdot}0; \tag{15a}$$

region 2, $$x=\frac{z-\text{dist1}}{\delta_p}; \tag{15b}$$

region 3, $$x=1{\cdot}0+\frac{z-\text{dist1}-\delta_p}{\text{dist2}}. \tag{15c}$$

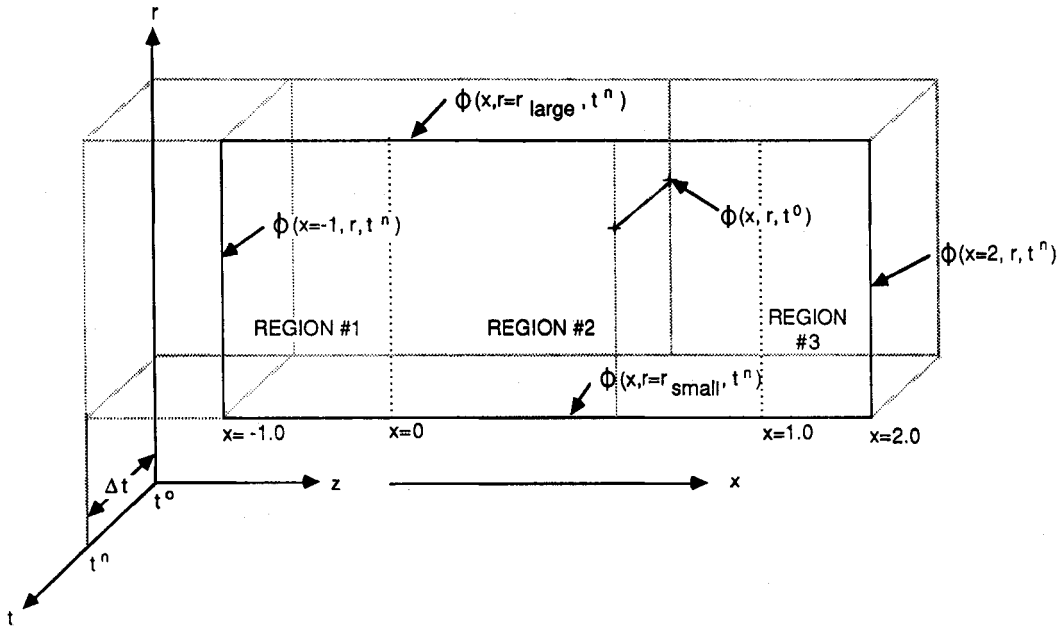

Figure 2. Dirichlet boundary conditions used in error analysis

Thus x has a different meaning in each region. The solution to this problem was found to be the specification of ϕ as $\phi(z, r, t)$ throughout all three regions instead. The meaning of z does not vary with region. The expressions for $R_{\text{anal}_\phi}(z, r, t)$ become identical to those given in Table II with all the xs physically replaced by zs, assuming all the xs in equations (7)–(13) are also replaced with zs. For applications which require only a Eulerian description, $\delta_p = 1$, $\bar{u} = u$ and $x = z$ throughout. Thus, for such applications it is preferable to use $\phi(x, r, t)$. For flow solutions with a strictly Lagrangian description, using $\phi = \phi(z, r, t)$ should prove easier. For the latter, however, either approach may be used.

During the iterative process of constructing equations (7)–(14), discrepancies were encountered between the computed and analytical values at various locations. Not knowing whether these discrepancies were due either to coding and discretization errors or to function ϕ selection, it was found necessary to break the problem down into smaller problems. References 6 and 7 give the details of the discretization of each of the source terms in Table I and break each $\bar{S}_\phi$ down into sub-expressions (such as vs1, vs2, vs3, vs4 and vs5 for $\bar{S}_v$, etc.). It was found convenient to calculate both analytical and numerical values corresponding to each of these sub-expressions for comparison. This enabled the causes of various discrepancies to be quickly pinpointed.

In addition, the solution algorithm was designed so that for most cases the primitive variables could be solved for numerically in a manner independent of all other variables. This was easily accomplished by prespecifying the analytical values of all other primitive variables at each solution nodal point and by then not recomputing the values of those not being solved for. Thus the discretization and coding of most of the primitive variables could be analysed one at a time. This and the specification of both the analytical and computed values of each source subterm enabled an exacting verification to be made of the code used for the analysis given in References 2–4 and 9.

DISCUSSION OF RESULTS

Several series of error test runs were conducted during the development of the solution code as a means of checking for mistakes both in the discretization of the governing equations and in the actual programming of the code. The first set of tests was made on the code representation of the untransformed equations for u, v, k, ε and T. In these tests the spacing was uniform for both the z- and r-co-ordinates. Afterwards, the code representation of the transformed equations for these same five primitive variables was tested with non-uniform spacing in the z-direction but with uniform spacing in the r-direction.

At a much later date, just prior to the final data runs for the analysis of the real world problems reported in References 2–4, another series of tests was conducted. The results of these tests are given in References 6 and 7. The rationale for this later round of tests was to ensure that no errors had been inadvertently inserted into the programme in the interim. For all these and earlier runs the pressure was specified as a constant and a simplified expression for temperature was used instead of that given in equation (12).

Reported herein are only the results of a series of tests conducted much more recently and which consider the influence of pressure gradients throughout the solution region.

The geometric values used in the formulation of the boundary conditions for these recent runs (see Figure 2) are as follows:

$$z_{x=0}=0{\cdot}974\text{ m},\quad r_{\text{small}}=1{\cdot}0144\text{ m},\quad r_{\text{large}}=1{\cdot}064\,24\text{ m},\quad \text{dist1}=0{\cdot}04\text{ m},\quad \text{dist2}=0{\cdot}003\,3333\text{ m}.$$

The time domain boundary conditions corresponding to the previous time step were specified for $\phi(x, r, t-\Delta t)$ using a time step $\Delta t=0{\cdot}000\,5263$ and a current time $t^n=1{\cdot}578\,95$ s. The value for Δt used is based[2] on 1/RPM and an RPM (revolutions per minute) of 1900. The t^n-value creates a $\delta_p(t)$ that gives the desired region 2 grid spacing for the test. This selection also affected in turn the specification of the error elimination constants C_6–C_{12} given earlier.

The error analysis algorithm was programmed in such a way so as to facilitate the testing of the code representation of one primitive variable at a time as well as any combination of primitive variables at a time. As mentioned, those variables not being tested had to be prespecified analytically owing to the fact that the governing equations are coupled.

The results of eight of the many runs conducted for the configuration given above are listed herein. All these runs are based on an 8×7 mesh (including boundary nodal points). First a series of individual variable runs for the primitive variables u, v, k, ε, T and P were made. It was found that the maximum computed percentage error over the entire solution field for each variable was less than 0·0139%. This is despite the fact that a maximum percentage error of the order of 0·1% would have been deemed acceptable for these individual runs. The maximum percentage errors for each of the primitive variables are: u, 0·013 29%; v, 0·0096%; k, 0·0041%; ε, 0·005 04%; T, 0·0139%; P, 0·0112%. The individual solution run for ε made use of the simultaneous solution for k. Similarly, the solution for P required the simultaneous solutions of u and v. The least accurate of these individual runs was found to be the solution for the energy equation. Results of this run (for T) are given in Table III to show the typical values one can expect for such a calculation. At the bottom of this table the computed values of temperature are repeated. Given in addition at the bottom of the table are the x- and r-co-ordinate values corresponding to each of the scalar solution nodal points. These are thus the same positions used for k, ε and P for both the individual and combined runs. A combined run for the variables u, v, k, ε and T resulted in maximum percentage errors of: u, 0·013 33%; v, 0·0099%; k, 0·0042%; ε, 0·0052%; T, 0·0137%. The primitive variable values obtained in this run were almost identical to those obtained for each of the individual runs for the same variables. In Table IV the computed values of u and v for this combined run are given with the x- and r-co-ordinate values corresponding to each of the

Table III. Energy equation data, individual run

i	j	T_{num}	T_{anal}	r_{num} * vol	r_{anal} * vol	%T error
3	2	764·94	764·89	76·4103	76·4119	0·006807
3	3	757·86	757·78	94·0932	94·0938	0·010857
3	4	747·75	747·65	79·7972	79·7990	0·013854
3	5	743·54	743·45	63·9459	63·9452	0·012093
3	6	736·30	736·24	82·2141	82·2148	0·007959
4	2	758·84	758·81	47·1051	47·1081	0·002863
4	3	751·68	751·64	58·0067	58·0092	0·005051
4	4	741·49	741·43	49·1971	49·1968	0·007993
4	5	737·25	737·20	39·4209	39·4228	0·006450
4	6	729·96	729·93	50·6871	50·6865	0·003980
5	2	750·18	750·16	56·8227	56·8260	0·002595
5	3	742·94	742·91	69·9750	69·9764	0·003829
5	4	732·62	732·58	59·3466	59·3465	0·006657
5	5	728·34	728·30	47·5557	47·5563	0·005380
5	6	720·97	720·94	61·1469	61·1441	0·003810
6	2	741·48	741·47	58·4559	58·4578	0·002387
6	3	734·15	734·13	71·9839	71·9863	0·003093
6	4	723·71	723·67	61·0491	61·0515	0·005760
6	5	719·38	719·35	48·9234	48·9228	0·004624
6	6	711·93	711·90	62·9017	62·9014	0·003592
7	2	732·73	732·72	60·1231	60·1258	0·002149
7	3	725·31	725·29	74·0419	74·0408	0·002449
7	4	714·75	714·72	62·7926	62·7945	0·004851
7	5	710·37	710·34	50·3204	50·3196	0·003798
7	6	702·84	702·81	64·6979	64·6977	0·003291
8	2	723·93	723·92	67·2849	67·2867	0·001661
8	3	716·42	716·41	82·8598	82·8594	0·001482
8	4	705·73	705·71	70·2746	70·2742	0·003122
8	5	701·30	701·29	56·3114	56·3136	0·002332
8	6	693·69	693·67	72·4052	72·4048	0·002499

	Temperature						
j	$i=3$	$i=4$	$i=5$	$i=6$	$i=7$	$i=8$	r
6	$7{\cdot}36\times10^2$	$7{\cdot}30\times10^2$	$7{\cdot}21\times10^2$	$7{\cdot}12\times10^2$	$7{\cdot}03\times10^2$	$6{\cdot}94\times10^2$	1·0140
5	$7{\cdot}44\times10^2$	$7{\cdot}37\times10^2$	$7{\cdot}28\times10^2$	$7{\cdot}19\times10^2$	$7{\cdot}10\times10^2$	$7{\cdot}01\times10^2$	1·0092
4	$7{\cdot}48\times10^2$	$7{\cdot}41\times10^2$	$7{\cdot}33\times10^2$	$7{\cdot}24\times10^2$	$7{\cdot}15\times10^2$	$7{\cdot}06\times10^2$	1·0064
3	$7{\cdot}58\times10^2$	$7{\cdot}52\times10^2$	$7{\cdot}43\times10^2$	$7{\cdot}34\times10^2$	$7{\cdot}25\times10^2$	$7{\cdot}16\times10^2$	0·9996
2	$7{\cdot}65\times10^2$	$7{\cdot}59\times10^2$	$7{\cdot}50\times10^2$	$7{\cdot}41\times10^2$	$7{\cdot}33\times10^2$	$7{\cdot}24\times10^2$	0·9948
x	−0·40000	0·00000	0·250000	0·50000	0·75000	1·00000	
z	0·97000	0·97400	0·97967	0·98533	0·99100	0·99667	

non-scalar solution nodal points. The values for the x- and r-co-ordinates given here follow from the use of the staggered grid arrangement described in Reference 3. A combined run for P and T was also conducted. As before for P, the simultaneous solutions of u and v were required. For this run the maximum percentage error for P remained unchanged from that of the individual run (0·0112%) but the maximum percentage error for T increased slightly to 0·025%. Also, as can be seen from Tables III and IV, both the x- and r-spacings for all these runs are non-uniform.

Figure 3 is a vector plot for the flow using the vector sum of the u- and v-velocity components in the vicinity of the scalar nodal points. The tail of each of these vectors shows the location of the

Table IV. Velocity field from simultaneous solution of equations for u, v, k, ε and T

	u-velocity					
j	$i=4$	$i=5$	$i=6$	$i=7$	$i=8$	r
6	1·51	1·53	1·55	1·56	1·58	1·0140
5	1·51	1·52	1·54	1·56	1·57	1·0092
4	1·50	1·52	1·53	1·55	1·57	1·0064
3	1·49	1·51	1·52	1·54	1·56	0·9996
2	1·48	1·50	1·52	1·53	1·55	0·9950
x	−0·20000	0·12500	0·37500	0·62500	0·87500	
z	0·97200	0·97683	0·98250	0·98817	0·99383	

	v-velocity						
j	$i=3$	$i=4$	$i=5$	$i=6$	$i=7$	$i=8$	r
6	−1·04	−1·05	−1·06	−1·06	−1·07	−1·07	1·0116
5	−1·04	−1·04	−1·05	−1·05	−1·06	−1·07	1·0078
4	−1·03	−1·03	−1·04	−1·04	−1·05	−1·06	1·0003
3	−1·02	−1·02	−1·03	−1·03	−1·04	−1·04	0·9972
x	−0·40000	0·00000	0·25000	0·50000	0·75000	1·00000	
z	0·97000	0·97400	0·97967	0·98533	0·99100	0·99667	

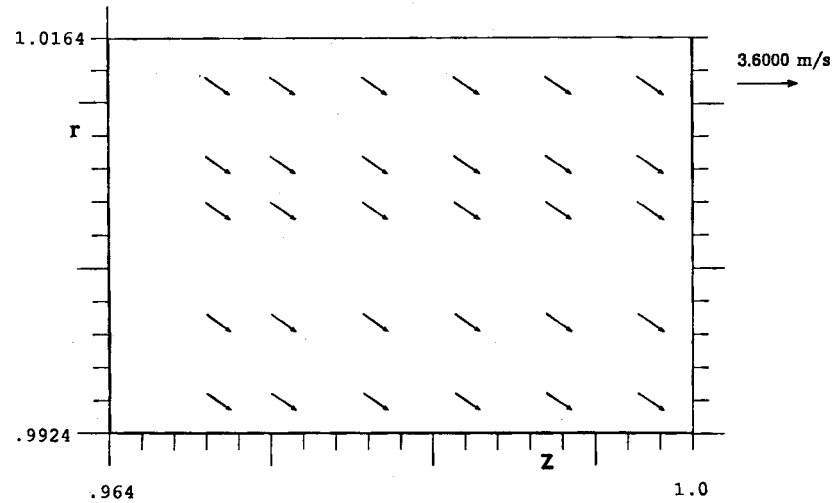

Figure 3. Velocity vector plot

corresponding scalar primitive variables. The magnitude of the arrows represents the vector sum of the u- and v-vectors having the same i- and j-indices. The locations of the true tails of each of the individual u- and v-vectors are the x- and r-values given in Table IV for each velocity. Figures 4–7 represent plots of isocontours of the primitive variables k, ε, T and P respectively. Because of the extremely high accuracy involved in the numerical solution, these five figures (Figures 3–7) represent both the analytical and numerical solutions of the governing equations for the Dirichlet boundary conditions given in Figure 2.

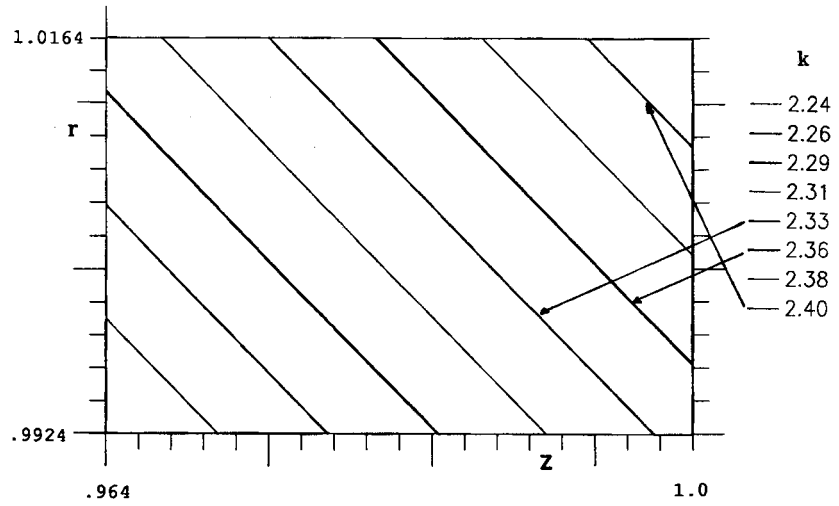

Figure 4. Turbulence kinetic energy distribution

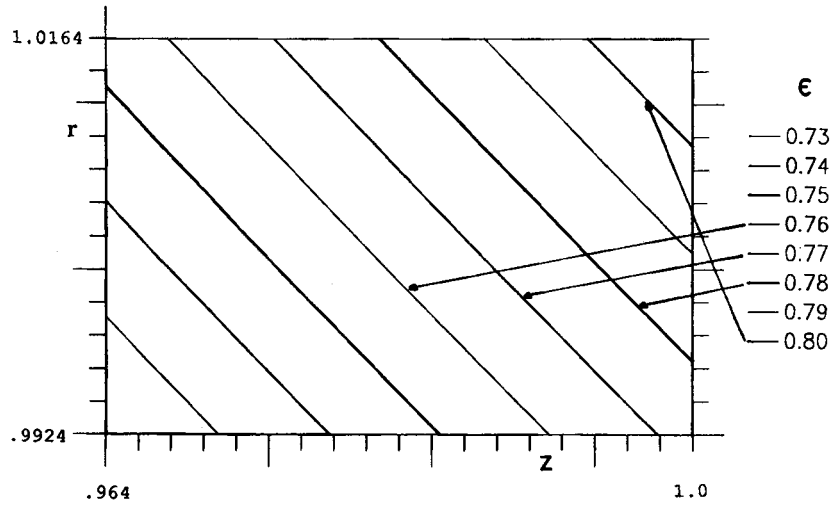

Figure 5. Turbulence kinetic energy dissipation rate distribution

Figure 3 makes it clear that the flow is oblique to the solution grid. An overlay of Figure 3 on each of Figures 4–7 makes it clear that a non-zero gradient exists for each of the dependent variables along the direction of flow everywhere in each of the primitive variable solution domains. These two conditions are the prerequisites for false diffusion to occur[8] if the Peclet numbers (P_m, m = e, w, n, s) of any of the mesh cells become large. As can be seen from the bottoms of Tables III and IV, the grid spacings in both the z- and r-directions have been kept sufficiently small. The largest P_m-value for any of the variables for the combined variable run given in Table IV is only 0·027. If values of P_m were not so constrained, one would not expect the excellent comparison obtained in this study with the use of the power-law spatial-differencing scheme for the numerical approximation of the convection–diffusion flux terms.

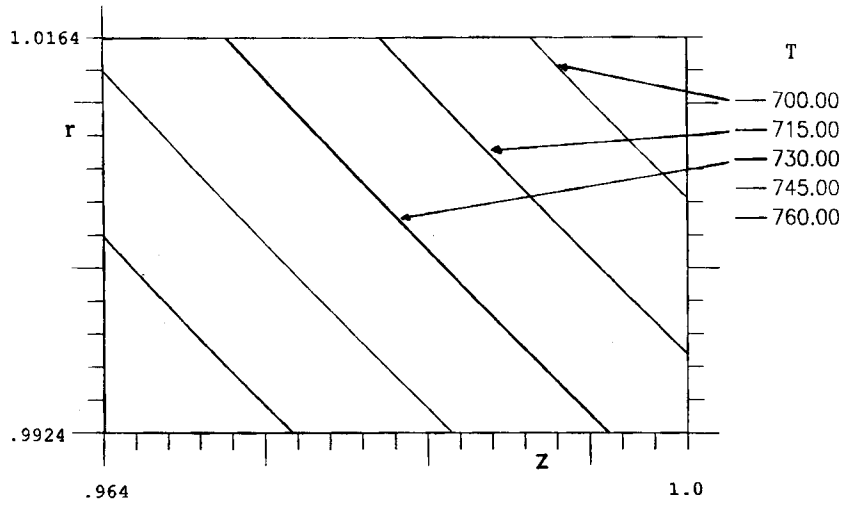

Figure 6. Temperature distribution

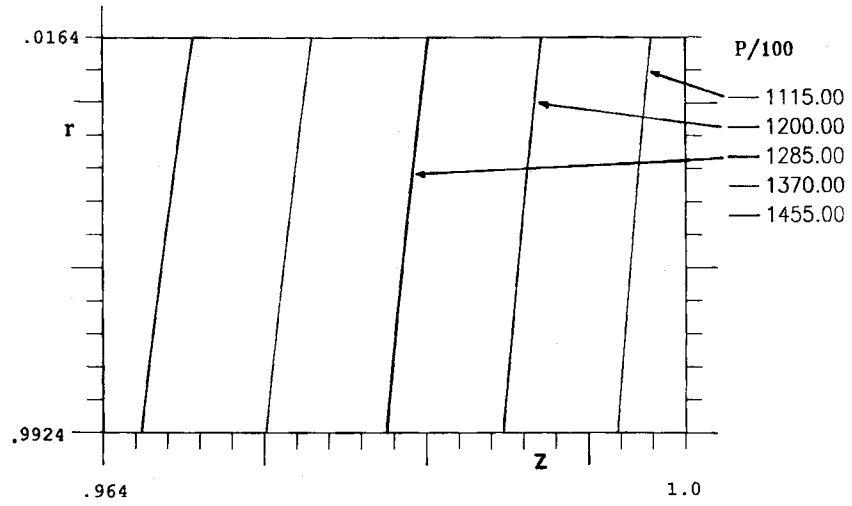

Figure 7. Pressure distribution

CONCLUSIONS

As can be seen from the data for both the individual and combined runs given in the previous section, the comparison between the numerically computed values of the various ϕs with the actual (analytical) values is excellent for all six primitive variables, both when they are computed individually and in combination. Such results point to the confidence that can be placed in numerical calculations for a set of very sophisticated governing equations, assuming the equation set accurately models the flow process. Also, these results demonstrate the viability of Shih's debugging procedure[5] to problems where a large set of complex governing equations applies. The procedure outlined herein has been demonstrated for fairly general governing equations. For

axisymmetric calculations which require modified versions of the governing equations, changes can easily be made to Table II on a term-by-term basis by either adding or subtracting the appropriate analytical expressions as necessary. For example, many turbulent fluid problems can be adequately described by a set of simpler governing equations which do not include the final expressions in each of the source terms given in Table I for u, v and ε. For such problems the deletion of the final expressions given in Table II for the source terms (S_ϕ) for u and v is all that is needed to correct Table II. No change in the source term for ε is necessary. Thus it can be seen that, without much additional effort, other researchers will be able to adapt this work to a variety of problems.

However, perhaps the most significant of the findings recorded herein is the fact that the same error elimination formulation may be used for both Eulerian and Lagrangian descriptions. This makes possible the application of this formulation, without modification, to flow field solutions which involve combined Eulerian–Lagrangian descriptions. Finally, this study validates the special matching procedure (reported in Reference 4) used to merge portions of the flow field having a Eulerian description with those having a Lagrangian description.

APPENDIX: NOMENCLATURE

a_m	coefficient of combined convective/diffusive flux through the designated wall of a control volume (m = N, S, E, W)
a_p	sum of coefficients of combined convective/diffusive flux through control volume walls
C	number equal to unity when solving using error analysis formulation and equal to zero otherwise
C_1, C_2, C_D, C_μ	constants of turbulence model (1·44, 1·92, 1·00 and 0·09 respectively)
C_6–C_{12}	constants used in error elimination procedure
C_p	specific heat at constant pressure (1·0 kJ kg^{-1} K^{-1})
dist1, dist2	axial lengths of solution regions 1 and 3 respectively
G, $\bar{G}$	generation of turbulence kinetic energy term (untransformed and transformed respectively)
H	differential operator defined by equation (4d) for the general primitive variable ϕ
i, j	indices in axial (x and z) and radial (r) directions respectively
k	turbulence kinetic energy
M	mass in a finite difference cell volume divided by the computational time increment
P	pressure
P_m	Peclet number (m = n, s, e, w) defined in Reference 3
Pr_l, Pr_t	laminar and turbulent Prandtl numbers (1·0 for both)
r	radial co-ordinate
R	gas constant (value for air used throughout)
S, $\bar{S}$	source terms in untransformed and transformed governing differential equations respectively
S_p	portion of integrated source term which is multiplied by ϕ_P
S_u	portion of integrated source term
t	time
T	temperature
u	axial velocity in Eulerian frame
$\tilde{u}$	axial velocity relative to moving co-ordinate frame (Lagrangian)

v	radial velocity
V	cell volume
x	non-dimensional axial co-ordinate
z	axial co-ordinate
z_p	Instantaneous distance equal to the combined axial lengths of regions 1, 2 and 3

Greek symbols

γ	a parameter (μ/Pr)
Γ	diffusivity
δ	increment
δ_p	instantaneous axial length of region 2 ($z_p - \text{dist1} - \text{dist2}$)
Δt	time increment
ε	dissipation rate of turbulence kinetic energy
μ_l, μ_t	laminar dynamic viscosity and turbulent viscosity respectively (μ_l is specified throughout as $1{\cdot}78 \times 10^{-5}\,m^2\,s^{-1}$)
μ_{eff}	effective viscosity ($\mu_l + \mu_t$)
ρ	density
σ_k, σ_ε	constants for turbulence kinetic energy and turbulence kinetic energy dissipation rate respectively (1·0 and 1·2 respectively)
τ	shear stress
ϕ	primitive variable (1, u, v, k, ε or T)
∇	divergence operator

Subscripts

eff	effective
l	laminar
n, s, e, w	cell boundary locations of finite difference grid
P, N, S, E, W	nodal points of finite difference grid
t	turbulent
ϕ	primitive variable (1, u, v, k, ε or T)

Superscripts

n	new time level
o	old time level

REFERENCES

1. A. D. Gosman and A. P. Watkins, 'A computer prediction method for turbulent flow and heat transfer in piston/cylinder assemblies'. *Symp. Turbulent Shear Flows*, Pennsylvania State University, April 1977, pp. 5.23–5.30.
2. D. A. Blank and T. M. Shih, 'Conjugate conduction–convection heat transfer model for four-stroke heat barrier piston engines'. *Numer. Heat Transfer A*, **15**, 357–382 (1989).
3. D. A. Blank and T. M. Shih, 'Hypergolic combustion model for four-stroke heat barrier pistons engines'. *Numer. Heat Transfer A*, **17**, 1–28 (1990).
4. D. A. Blank, 'Conjugate conduction–convection heat transfer model for the valve flow-field region of four-stroke piston engines'. *Numer. Heat Transfer A*, **18**, 283–308 (1990).
5. T. M. Shih, 'A procedure to debug computer programs'. *Int. j. numer. methods eng.*, **21**, 1027–1037 (1985).
6. D. A. Blank, 'Numerical heat transfer model for a heat-barrier-piston engine with hypergolic combustion', *Ph.D. Thesis*, University of Maryland, College Park, MD, 1985.
7. D. A. Blank, 'Numerical heat transfer model for a heat-barrier-piston engine with hypergolic combustion', *U.S. Naval Academy, Engineering and Weapons Rep. EW-8-86*, February 1986.
8. S. V. Patankar, *Numerical Heat Transfer and Fluid Flow*, Hemisphere, Washington, DC, 1980, pp. 90–109, 152–153.
9. D. A. Blank, 'The modified discretized-intensity based split radiation calculation procedure for use in full simulation studies of combustion in axisymmetric piston engines'. *Numer. Heat Transfer A*, **22** (1992).